

# **Effect of noncondensable gas on Steam Condensation in Passive containment cooling tube**

N. K. Maheshwari, P.K. Vijayan and D. Saha  
Reactor Engineering Division  
Bhabha Atomic Research Centre  
Trombay, Mumbai 400 085  
Email: nmahesh@apsara.barc.ernet.in

## **ABSTRACT**

A theoretical model has been developed to study the local heat transfer coefficient of a condensing vapour in the presence of a noncondensable gas, where the gas/vapor mixture is flowing downward inside a vertical tube. The two-phase heat transfer is analysed assuming an annular flow pattern with a liquid film at the tube wall and a turbulent gas/vapour core. The gas-vapour core is modeled using the analogy between heat and mass transfer. The model incorporates Nusselt equation with McAdams modifier and Blangetti model for calculating the film heat transfer coefficient. Moody and Wallis correlations were used to account for film waviness effect on gas/vapor boundary layer. The suction effect due to condensation, effects of developing flow and property variation in the gas phase are also considered. A comparative study of heat transfer coefficient has been made with various models to account for condensate film resistance and condensate film roughness. Results show that the condensation heat transfer coefficient is higher than the film heat transfer coefficient for very high Reynolds number.

## **1. INTRODUCTION**

Containment of a nuclear reactor is a key component of the mitigation part of the defence in depth philosophy, since it is the last barrier designed to prevent large radioactive releases to the environment. While containments of current Nuclear Power Plants (NPPs) are able to meet the objectives they have been designed for in the frame of defence in depth approach, many improvements are proposed by designers to further reduce the probability of releases to the environment under accident situations. One of the proposed systems is Passive Containment Cooling System (PCCS) to provide safety-grade ultimate heat sink for preventing the containments exceeding its design pressure. A number of PCCS has been proposed for a large variety of advanced reactors. PCCS with immersed condensers (IC) [1] for long-term containment cooling is being considered as one of the alternatives in Indian Advanced Heavy Water Reactor. The function of IC is to condense the steam released into the containment following a loss of coolant accident. As these ICs are immersed in a pool of water inside the containment, the heat transfer from steam-noncondensable gas takes place through IC to the water pool. In performing this function, the IC must have the capability to remove sufficient energy from the reactor containment in order to prevent ground leakage from the containment. After a typical postulated loss of coolant accident, the steam-air mixture flows into IC where condensation of steam takes place. In IC the heat transfer coefficient varies greatly along the length of the tube. The progressively increasing air mass fraction and decreasing velocity due to condensation of

steam mainly cause the decrease in heat and mass transfer with distance down the tube. Knowledge of variation of local heat transfer coefficient is necessary in order to predict PCCS system response and to optimize the IC design.

For theoretical analysis of condensation of vapour in presence of a non-condensable gas, the heat and mass transfer analogy models follow the general methodology of Colburn and Hougen [2]. In 1934, Colburn and Hougen proposed the theory that condensation mass transfer is controlled by diffusion across a thin film at which the accumulation of noncondensable gas occurs. Their methodology is based on the heat balance at the liquid/gas interface between the heat transfer through the vapour/gas boundary layer and the heat transfer through the condensate film. The heat transfer through vapor/gas mixture is made up of two components, the sensible heat transfer because of temperature difference between bulk vapour/gas mixture and interface and the latent heat given up by the condensing vapour. Separate models for sensible and latent heat fluxes were used. Several attempts have been made to simplify methods for estimating the heat and mass transfer. Peterson et al. [3] had developed a mechanistic model by combining the thermal resistance of the liquid and gas/vapor sides in series to evaluate the total heat transfer coefficient. The heat transfer coefficient of the liquid film was estimated using the Blangetti's correlation [4]. The mass transfer and the sensible heat transfer in the gas/vapor side were estimated by the Dittus-Boelter equation, using the heat and mass transfer analogy. They derived an empirical method for estimating condensation heat transfer based on equivalent thermal conductivity due to condensation, derived from thermodynamic relationships with several additional assumptions. By this way, the mass transfer problem was recast as a heat transfer problem by defining the condensation thermal conductivity. The correlations however, involve a large number of empirically adjusted parameters, which are attributed to the effects of mist formation, surface roughness due to film waviness and suction effect due to condensation. It involves an iterative multistep procedure and incorporates a search for the variation of the bulk and interface concentration. The predictions are compared with the experimental data from Kageyama [5], Vierow [6], Ogg [7] and Siddique [8]. A similar approach was employed by Siddique et al. [9] who analyzed two phase heat transfer using an annular flow pattern with a liquid film at the wall and a turbulent gas/vapour core. The liquid-phase heat transfer was modeled by multiplying the value from the Nusselt's analysis by a factor of 1.28. Emphasis was also placed on including the effects of developing flow, condensate film roughness, suction effect (using correlation given by Kays and Moffat [10]) and property variation in gas phase. The model was applied on helium/steam and air/steam mixtures separately and the theoretical results were compared with the experimental results from Siddique et al. [8]. Ghiaasiaan et al. [11] used a two-fluid model to analyze the condensation process in presence of air as the noncondensable in a co-current two-phase channel flow. The predicted results are also compared with the experimental data of Vierow [6], Ogg [7] and Siddique [8]. Hassan et al. [12] implemented the model proposed by Kageyama et al. for condensation in presence of the noncondensable [13] in RELAP5/MOD3, which is a computer code used for safety analysis of nuclear reactors. The theoretical results are compared with the experimental data of Siddique [8]. Herranz et al. [14] developed a model in which the new methods to estimate the film thickness was incorporated. They rederived the effective condensation thermal conductivity by taking the Peterson's fundamental theory into account with new assumptions. In place of Dittus-Boelter correlation for heat transfer, the Gnielinski correlation [15] was applied. The model considers the effects of high mass flux, mist and film roughness. Recently, No et al.

[16] had developed a non-iterative method in which the unknown interfacial temperature need not be assumed beforehand.

In the present paper, a theoretical model based on iterative method for vertical in-tube condensation in presence of noncondensable gas has been developed. The analysis accounts for the effect of waviness. Different models for film heat transfer coefficient have been considered for the analysis. A computer code based on this model has been developed to predict heat transfer along the length. At the inlet, the mixture temperature, noncondensable mass fraction and velocity are provided as input data. The other relevant parameters like total pressure, wall temperatures, etc. are also specified. The interface temperature is unknown and lies between the wall temperature and the bulk vapor/gas temperature. An iterative scheme based on heat balance at the liquid/vapor-gas interface has been used for calculating the local heat transfer coefficient, mass of the steam condensed and the interface temperature along the length of the tube. A comparison of heat transfer coefficient predicted using these models with experimental data is also given in the paper.

## 2. THEORETICAL MODEL

In general, during forced in-tube condensation of a vapour in the presence of a noncondensable gas, the condensed liquid flows as an annular film adjacent to the cooled tube wall, while the uncondensed vapour/gas mixture flows in the core of the tube. The high density difference between the condensed liquid and the gaseous core leads to a very low liquid volumetric fraction and together with the shear force of the gaseous core, an annular flow pattern is maintained over most of the condensing length. Figure 1 depicts schematically the model considered for analysis. The inside wall of the tube is at a prescribed temperature  $T_w$ , lower than the saturation temperature of the steam, and therefore condensation takes place on the wall surface to begin with. Eventually, a condensate film forms, whose thickness,  $\delta$ , is a function of the position along the flow direction. The gas/steam mixture has a given inlet bulk temperature  $T_b$ , and a corresponding inlet concentration of the noncondensable gas  $W_{nc,b}$  at the given pressure. At the liquid and gas/vapour interface, the temperature  $T_i$  and the gas mass fraction  $W_{nc,i}$  are unknown and must be determined from the analysis. The analysis of the condensation in the presence of a noncondensable gas typically involves a heat balance at the liquid/gas interface. However, models for the condensate film and gas/vapour are linked and simultaneously solved for the heat and mass transfer rates.

### 2.1 Fundamentals of heat and mass transfer at gas/vapour boundary layer

The heat transfer through the gas/vapour boundary layer consists of the sensible heat transfer and the latent heat given up by the condensing vapour. Hence the total heat transfer rate from the gas/vapour side to an elemental area of the interface can be written as,

$$dQ = dm_{\text{cond}} H_{fg} + h_g dA (T_b - T_i) \quad (1)$$

which must be equal to the rate of heat transfer from the interface through condensate film to the tube wall, i.e.

$$dQ = h_f dA (T_i - T_w) \quad (2)$$

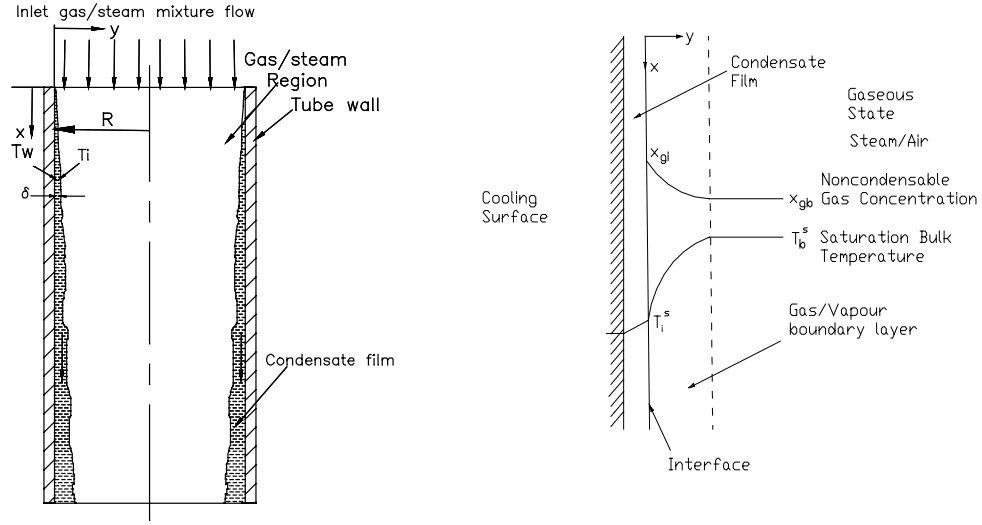


Fig.1 Schematic Illustration of the Model

After dividing by  $dA$  in both equations and equating the Eq.(1) and Eq.(2) we get,

$$h_f (T_i - T_w) = m''_{cond, x} H_{fg} + h_g (T_b - T_i) \quad (3)$$

where  $h_g$  is the heat transfer coefficient for sensible heat transfer from the gas phase to liquid film. The condensation heat transfer coefficient,  $h_{cond}$  can be defined as

$$h_{cond} (T_b - T_i) = m''_{cond, x} H_{fg} \quad (4)$$

From Eq. (3) we obtain,

$$\begin{aligned} h_f (T_i - T_w) &= h_{cond} (T_b - T_i) + h_g (T_b - T_i) \\ &= (h_{cond} + h_g) (T_b - T_i) \end{aligned} \quad (5)$$

The total heat transfer from the tube wall may be expressed by,

$$dQ = h_{tot} dA (T_b - T_w) \quad (6)$$

The overall heat transfer coefficient  $h_{tot}$  is given by,

$$h_{tot} = \left[ \frac{1}{h_f} + \frac{1}{h_{cond} + h_g} \right]^{-1} \quad (7)$$

The sensible heat transfer coefficient from gas phase to the liquid film  $h_g$  is found as follows,

$$h_g = Nu_x \frac{k}{d} \quad (8)$$

To find  $m''_{cond}$  a mass balance at the interface is done to yield the following equation,

$$m''_{cond} = \left[ -\rho D \frac{\partial W_v}{\partial y} \right]_i + W_{v,i} (m''_{tot})_i \quad (9)$$

As the condensate surface is impermeable to the noncondensable gas. So,  $m''_{tot} = m''_{cond}$  and Eq. (9) can be simplified as,

$$\begin{aligned} m''_{cond} &= \left( -\rho D \frac{\partial W_v}{\partial y} \right)_i / (1 - W_{v,i}) \\ &= \rho h_m \frac{(W_{v,b} - W_{v,i})}{(1 - W_{v,i})} \end{aligned} \quad (10)$$

where  $h_m$  is the mass transfer coefficient and by definition  $h_m = D \frac{\partial W_v}{\partial y} \frac{1}{(W_{v,b} - W_{v,i})}$ .

Noting that  $W_{v,b} + W_{nc,b} = W_{v,i} + W_{nc,i} = 1$ , the above equation can be recast, in terms of Sherwood number ( $h_m d/D$ ), as

$$Sh_x = \frac{m''_{cond,x} d}{\rho D} \frac{W_{nc,i,x}}{(W_{nc,i,x} - W_{nc,b,x})} \quad (11)$$

For the calculation of various heat transfer coefficients defined above following models are considered. The necessary modifications to take into account the condensate film roughness effect, suction effect and developing flow effect on heat and mass transfer are discussed by modifying Nusselt number and Sherwood number.

## 2.2 Condensate film model

In pure vapour condensation, the condensate film provides the only heat transfer resistance. If a small amount of a noncondensable gas is present, then the resistance to heat transfer in the gas/vapour boundary layer gets added to the condensate film resistance. The heat transfer coefficient of the condensate film is calculated as the ratio of condensate conductivity and film thickness. Under forced flow conditions, the resistance of the condensate film reduces because of thinning, rippling and waviness, and early transition to a turbulent flow regime of the condensate film. Corradini [17] found that the film heat transfer resistance did not significantly affect the overall heat transfer resistance in the presence of noncondensables. Hence, Siddique et al. [9] thought that elaborate

improvements to the Nusselt film analysis are not necessary. But in this analysis, it has been thought that by increasing the inlet Reynolds number of the mixture, the resistance to heat transfer in gas/vapor interface may not be dominating particularly at high gas/vapor Reynolds number. In that case, it is necessary to use a proper heat transfer model to calculate the resistance in the condensate film. To calculate the heat transfer in the condensate film two models are considered in the present analysis.

In the first model the condensate film heat transfer coefficient is given as,

$$h_f = \beta \frac{k_l}{\delta(x)} \quad (12)$$

The factor  $\beta$  modifies Nusselt equation to account for the increase in heat transfer as a result of waviness and rippling. The value of  $\beta$  is 1.28, as suggested by McAdams [18]. Siddique et al. [9] have used this multiplier throughout the length of the tube. In the analysis carried out by them the heat transfer coefficient estimated in the initial small length is higher as compared to the experimental data. Hence, in the present analysis, the factor  $\beta$  is applied when condensate film Reynolds number is more than 30.

After incorporating Nusselt assumptions, the local velocity profile [8] of the condensate film, in terms of coordinates of the system (figure 1), is given by

$$u_1(y) = \frac{g(\rho_l - \rho_v)\delta^2}{\mu_l} \left[ \frac{y}{\delta} - \frac{1}{2} \left( \frac{y}{\delta} \right)^2 \right] \quad (13)$$

Using this equation, the local condensate flow rate can be obtained as

$$m_{\text{cond}}(x) = \int_0^{\delta(x)} 2\pi \rho_l u_1(y) (R - y) dy \quad (14)$$

From Eq.(13) and Eq.(14), the local condensate flow rate can be obtained as

$$m_{\text{cond}}(x) = \frac{2\pi g \rho_l (\rho_l - \rho_v)}{\mu_l} \left[ \frac{R\delta^3}{3} - \frac{5\delta^4}{24} \right] \quad (15)$$

This equation is rederived, as the equation reported by Siddique et al. [8] was dimensionally inconsistent. At any axial position  $x$ , knowing the local condensate flow rate  $m_{\text{cond}}(x)$ , the local film thickness can be calculated by solving Eq. (15).

The second model used to calculate the heat transfer coefficient in the condensate film is Blangetti et al. [4] model. The model provides a weighted correction to the laminar Nusselt film solution. The Nusselt theory neglects interfacial shear and convective effects leading to a linear temperature distribution in the condensate film. While, here the condensate film thickness  $\delta$  depends on the local mass flow and the interfacial shear stress  $\tau_g$ ,

$$\Gamma = \frac{g\rho_1(\rho_1 - \rho_g)}{3\mu_1} \delta^3 + \frac{\rho_1\tau_g}{2\mu_1} \delta^2 \quad (16)$$

The shear stress exerted by the gas/vapor mixture on the condensate film is

$$\tau_g = f\rho_1 \frac{v_g^2}{2} \quad (17)$$

where  $v_g$  is gas velocity and  $f$  is a friction factor determined from graphical information provided by Blangetti et al. [4].

For a given condensate flow rate and interfacial shear, the laminar film thickness can be determined from Eq. (16), which can be nondimensionalized with the following substitutions

$$L = \left( \frac{\mu_1^2}{\rho_1^2 g} \right)^{1/3}, \quad \text{Re}_f = \frac{\Gamma}{\mu_1}, \quad \tau_g^* = \frac{\tau_g}{g\rho_1 \left( 1 - \frac{\rho_g}{\rho_1} \right) L}, \quad \delta^* = \frac{\delta}{L} \quad (18)$$

The film thickness is given by

$$\frac{\text{Re}_f}{1 - \frac{\rho_g}{\rho_1}} = \frac{\delta^{*3}}{3} + \frac{\tau_g^* \delta^{*2}}{2} \quad (19)$$

Blangetti et al. [4] extended the Rohsenow model [19] which predicts the Nusselt number over a vast range of film Reynolds numbers  $\text{Re}_f$ . Blangetti et al. suggest the existence of a transition region between laminar and turbulent film behaviour. In their model, the local Nusselt number  $\text{Nu}$  is written as

$$\text{Nu}_x = \frac{h_f L}{k_1} = (\text{Nu}_{x, \text{la}}^4 + \text{Nu}_{x, \text{tu}}^4)^{1/4} \quad (20)$$

From Nusselt theory [4], the local laminar film Nusselt number  $\text{Nu}_{x, \text{la}}$  is given by

$$\text{Nu}_{x, \text{la}} = \frac{1}{\delta^*} \quad (21)$$

Where  $\delta^*$  comes from the solution of Eq. (19). The local turbulent film Nusselt number  $\text{Nu}_{x, \text{tu}}$  was correlated as

$$\text{Nu}_{x, \text{tu}} = a \text{Re}_f^b \text{Pr}^c (1 + e\tau_g^* f) \quad (22)$$

where table 1 gives values for the coefficients  $a$ ,  $b$ ,  $c$ ,  $e$ ,  $f$ .

Table 1: Coefficient for the calculation of local condensate film Nusselt numbers

Coefficient	$\tau_g^*=0$	$0<\tau_g^*<5$	$5<\tau_g^*<10$	$10<\tau_g^*<40$
a	0.008663	0.008663	0.02700	0.04294
b	0.3820	0.3820	0.2071	0.09617
c	0.5689	0.5689	0.5000	0.4578
e	-	0.1450	0.4070	0.6469
f	-	0.5410	0.4200	0.4730

### 2.3 Film roughness considerations

As condensation proceeds along the tube, the laminar annular film becomes turbulent, rough and wavy, especially in the forced convection case, and this pattern is maintained over most of the condensing length. Film roughness increases the heat transfer from the gas phase by influencing the turbulence pattern close to the interface and disrupting the gaseous laminar sublayer. Using the corrections suggested by Norris [20] for the roughness of the heat transfer surface,

$$Nu_{or,x} = Nu_{os,x} \left( \frac{f_r}{f_s} \right)^n \quad \text{where } n = 0.68 Pr^{0.215} \quad (23)$$

$$Sh_{or,x} = Sh_{os,x} \left( \frac{f_r}{f_s} \right)^n \quad \text{where } n = 0.68 Sc^{0.215} \quad (24)$$

$$\text{and } f_s = 0.0791 Re^{-0.25} \quad (25)$$

Two models are considered for estimating the roughness of the condensate film. In the first model, the wavy condensate film is treated as the rough wall. Hence, rough wall friction factor calculated by Moody correlation [21] given below is applied

$$f_r = 1.375 \times 10^{-3} \left[ 1 + 21.544 \left( \frac{2\varepsilon}{d} + \frac{100}{Re} \right)^{1/3} \right] \quad (26)$$

Where Re is gas/vapour mixture Reynolds number. The friction factor  $f_r$  increases as the surface roughness increases. A conservative assumption of  $\varepsilon$  being equal to half of the film thickness  $\delta$  is chosen, as suggested by Siddique et al. [9]. For laminar flow, the condensate film roughness has little effect. Therefore, no correction is applied for laminar flow.

In the second model, to calculate the interfacial shear stress, the friction factor  $f_r$  is calculated using the Wallis [22] correlation for interfacial friction in the vertical annular flow

$$f_r = f_s \left( 1 + 300 \frac{\delta}{d} \right) \quad (27)$$

## 2.4 Suction effect considerations

The condensation process leads to a thinning of the gas/vapour boundary layer, which is called suction effect. This means that at the interface, the velocity component normal to the wall is not zero, and the correlations used to calculate heat and mass transfer, must take this into account. Kays and Moffat [10] experimentally obtained a correlation for sucked boundary layer, which is as follows,

$$\frac{St}{St_0} = \ln \frac{(1 + B_h)}{B_h} \quad (28)$$

Where Stanton number,  $St = \frac{Nu}{RePr}$

$St/St_0$  defines the ratio of Stanton number with suction to that without suction at the same Reynolds numbers and  $B_h = m''_{cond}/G^\infty St$  is called suction parameter. Eq. (28) can be recast as,

$$Nu_x = \left[ \exp \left( \frac{m''_{cond,x} Re_x Pr}{G^\infty Nu_{ox}} \right) - 1 \right]^{-1} \left[ \frac{G^\infty}{m''_{cond,x} Re_x Pr} \right]^{-1} \quad (29)$$

Using the analogy between heat and mass transfer, Eq.(29) can be written as,

$$Sh_x = \left[ \exp \left( \frac{m''_{cond,x} Re_x Sc}{G^\infty Sh_{ox}} \right) - 1 \right]^{-1} \left[ \frac{G^\infty}{m''_{cond,x} Re_x Sc} \right]^{-1} \quad (30)$$

In equations (29) and (30)  $Nu_{ox}$  and  $Sh_{ox}$  denote the respective local Nusselt number and Sherwood number without suction which is modeled using the Gnielinski correlation [15] given below

$$Nu_{o,x} = \left[ \frac{(f_s/2)(Re - 1000)Pr}{1 + 12.7(f_s/2)^{1/2}(Pr^{2/3} - 1)} \right] \quad (31)$$

$$Sh_{o,x} = \left[ \frac{(f_s/2)(Re - 1000)Sc}{1 + 12.7(f_s/2)^{1/2}(Sc^{2/3} - 1)} \right] \quad \text{for } 2300 \leq Re \leq 5 \times 10^6 \quad (32)$$

$$Nu_{o,x} = 3.66 \quad \text{and} \quad Sh_{o,x} = 3.66 \quad \text{for } Re \leq 2300$$

Combining Eq.(11) and Eq. (30) we can get  $m''_{cond,x}$  as follows

$$m''_{\text{cond},x} = \frac{G^\infty \text{Sh}_{\text{ox}}}{\text{Re}_x \text{Sc}} \left[ \ln \left\{ 1 + \frac{\text{Re}_x \text{Sc} D \rho (1 - \omega)}{G^\infty d} \right\} \right] \quad (33)$$

Where,  $\omega$  is the ratio of the noncondensable gas mass fraction in the bulk to that at the liquid/gas interface.

## 2.5 Developing flow considerations

As most of the heat transfer takes place in the first part of the condenser tube, it may be important to consider the developing flow effects in the heat and mass transfer model. For an initial conservative estimate of the heat transfer rate, it was assumed that the temperature and concentration profiles develop simultaneously in the presence of a previously developed velocity field. Reynolds et al. [23] suggested the following correlations for the thermal entrance zone,

$$\text{Nu}_{\text{ot},x} = \text{Nu}_{\text{o},x} \left[ 1 + \frac{0.8(1 + 7 \times 10^4 \text{Re}_x^{-3/2})}{x/d} \right] \quad (34)$$

$$\text{and } \text{Sh}_{\text{ot},x} = \text{Sh}_{\text{o},x} \left[ 1 + \frac{0.8(1 + 7 \times 10^4 \text{Re}_x^{-3/2})}{x/d} \right] \quad (35)$$

Where  $x$  is the distance from the tube inlet. The subscript 'ot' represents the effect of thermal length without suction effect.

## 3. EXPERIMENTAL DATA

There are a number of experimental studies on the condensation of a vapour inside the tube in the presence of noncondensables. Some selected sets of test data from Maheshwari et al. [24], Siddique et al. [8] and Tanrikut et al. [25] are taken for the comparison of the results obtained from the present model.

Table 2 Test section characteristics

Characteristics	Maheshwari [24]	Siddique [8]	Tanrikut [25]
Material of test tube	SS	SS	SS
Tube length ( m )	1.7	2.54	2.15
Cooled segment of the tube ( m )	1.6	2.44	2.15
Inner diameter ( m )	0.04276	0.046	0.033
Thickness ( m )	0.00277	0.0024	0.003

Table 3 Test inlet conditions

Reference	Case no.	Pressure (Pa)	Steam flow rate (kg/s)	Non-condensable mass fraction (%)	Mixture Reynolds number
Maheshwari	E19701	266000.0	0.004	11.5	9755
	E19704	266000.0	0.004	23	10549
Siddique	RUN # 47	214238.6	0.008863	9.8	18873
	RUN # 52	221140.6	0.008635	35.4	22733
Tanrikut	RUN-6.4.1	390600.0	0.01526	52	45195
	RUN-4.4.1	398200.0	0.02987	27.8	85898

The important geometric characteristics of the test sections are provided in Table 2. The test sections in these experiments were circular, vertical, metallic tubes. In Maheshwari's experiment the tube outer surface was cooled by natural convection of water in a pool while in Siddique and Tanrikut experiments the tube was cooled by a forced flow of water inside cooling jacket. The condensing mixture flowed downward in the channel while the coolant in the jacket flowed upward. The test data selected for analysis are summarized in Table 3. In these tests, air is the noncondensable and saturated steam is the condensing fluid. These tests cover a wide range of Reynolds number from 9755 to 85898 and air mass fraction from 9% to 60%.

#### 4. RESULTS AND DISCUSSIONS

A comparative study of various local heat transfer coefficients (condensate film, condensation, sensible and total heat transfer coefficients) and steam flow along the length of the tube is given in the following sections. The various models for condensate film heat transfer and film roughness described earlier are used for the theoretical studies. Comparison with experimental data is also presented in the sections given below.

##### 4.1 Total heat transfer coefficient

For all the cases given in table 3, figures 2 to 7 show the variation in the total heat transfer coefficient along the length of the tube. The total heat transfer coefficient has been estimated using the theoretical model with McAdams modifier and Blangetti model for heat transfer in the condensate layer, and Moody and Wallis correlations for accounting the condensate film roughness effect on the condensation and sensible heat transfer coefficients. From these figures it is found that the total heat transfer coefficient estimated with Blangetti model and Wallis correlation is higher as compared to that estimated with McAdams Modifier and Moody correlation and with Blangetti model and Moody correlation.

It can be seen that the total heat transfer coefficients estimated with McAdams modifier and Moody correlation and with Blangetti model and Moody correlation are more or less same except in fig.7. The comparison of total heat transfer coefficient further shows that theoretical heat transfer coefficient estimated with all the models matches well with the experimental data except in fig. 7. The analysis for all the cases show that the heat transfer

coefficient decreases sharply at the initial length and then slowly as the mass fraction of noncondensable gas increases along the length.

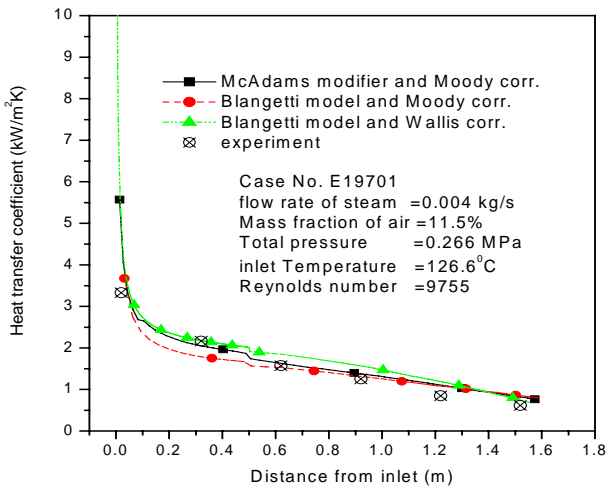


Fig 2 Variation of total heat transfer coefficient along the length of the tube

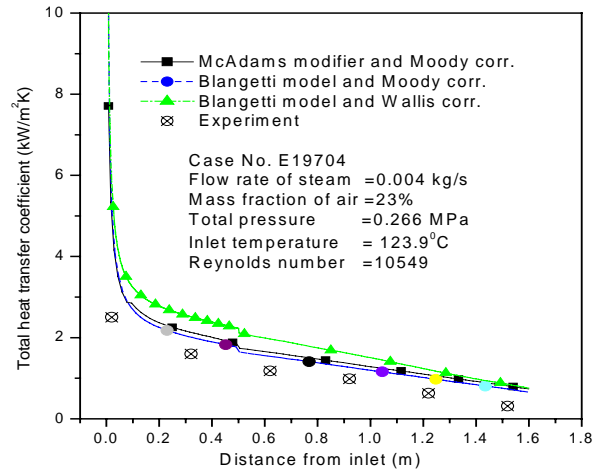


Fig 3 Variation of total heat transfer coefficient along the length of the tube

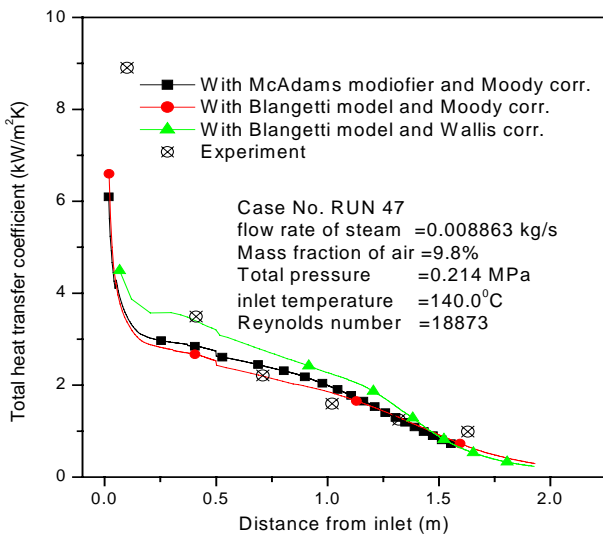


Fig 4 Variation of total heat transfer coefficient along the length of the tube

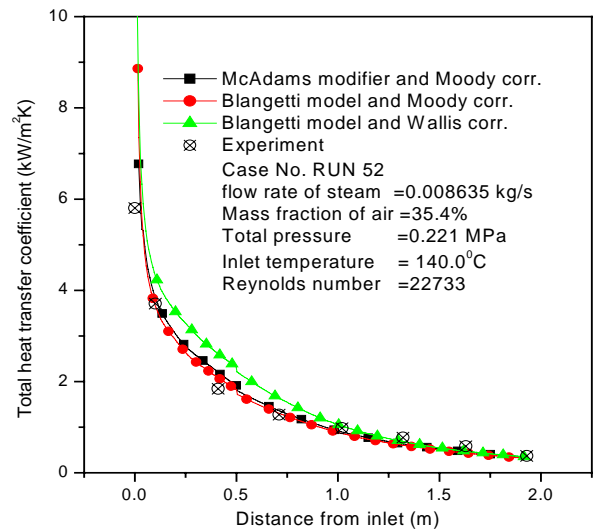


Fig 5 Variation of total heat transfer coefficient along the length of the tube

Figure 8 shows the comparison between heat transfer coefficient estimated by theoretical model with McAdams Modifier and Moody correlation and with Blangetti model and Wallis correlation and experimental data collected by Maheshwari et al. [24]. The root mean square error in case of theoretical model with McAdams modifier and Moody correlation with experimental data is 46% while it is 64% in case of theoretical model with Blangetti model and Wallis correlation. The deviation is higher at the inlet of the tube due to the low wall subcooling.

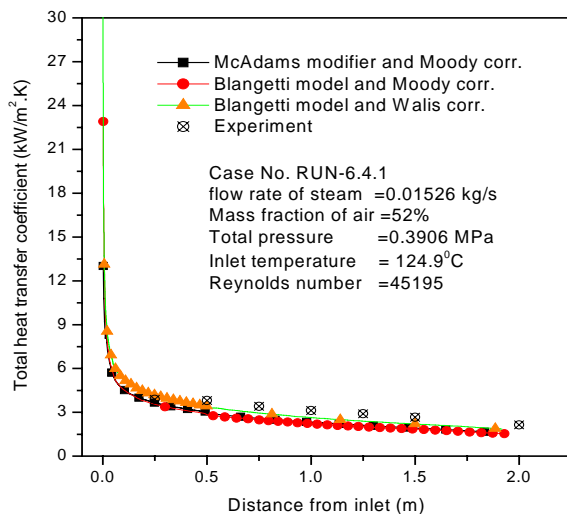


Fig 6 Variation of total heat transfer coefficient along the length of the tube

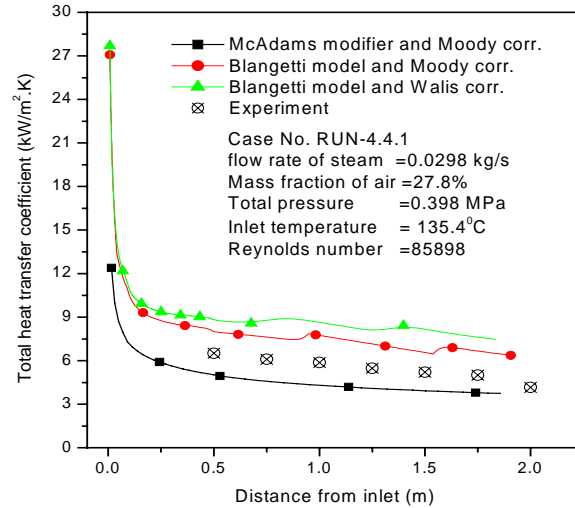


Fig 7 Variation of total heat transfer coefficient along the length of the tube

From figures 2 and 3, the experimental local heat transfer coefficient is found to be higher for the case with lower air mass fraction. The effect of inlet Reynolds number is not significant on local heat transfer coefficient due to low difference in inlet Reynolds numbers in both the cases. Comparing Figs. 2 and 4, the local heat transfer coefficient is always found to be higher for the case with higher Reynolds number. The inlet mass fraction for both the cases is only marginally different. In fig. 6, with inlet Reynolds number of 45195 and air mass fraction 52%, the local heat transfer coefficient is always higher than that of the cases given in figs. 2 to 5. It is expected that the increase in Reynolds number will cause increase in heat transfer coefficient while the increase in air mass fractions will cause reduction in heat transfer coefficient. However, the effect of Reynolds number on heat transfer is more compared to the effect of the inlet air mass fraction. This may be due to the higher turbulence in the gas/vapor boundary layer.

#### 4.2 Local condensate flow rate

To study the PCCS response, it is necessary to know the amount of steam condensed in the tubes of the immersed condenser. This will influence the pressure and temperature of the containment of the reactor. Hence, the comparison of steam flow inside the tube with various models has been given in figures 9 to 12. It can be inferred from the figures that the condensation of vapor with Blangetti model and Wallis correlation is higher as compared to the model with Blangetti model and Moody correlation and model with McAdams Modifier and Moody correlation. It can be also seen from fig. 9 to 12 that the difference in the steam flow rate estimated with McAdams modifier and Moody model and with Blangetti and moody models is marginal. From figure 13, the mass flow of steam is found to be reduced steeply with Blangetti model and Wallis correlation and with Blangetti model and moody correlation. A comparison of steam flow inside the tube between the experimental data collected by Maheshwari et al. [24] and the theoretical models is shown in fig. 14. The rms error in case of theoretical model with McAdams modifier and Moody correlation with experimental data is 12.5% while it is 16.7% in case of theoretical model with Blangetti model and Wallis correlation.

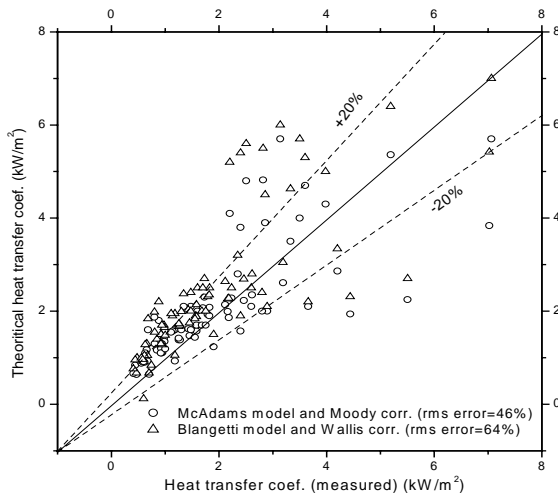


Fig. 8 Comparison between experimental and theoretical heat transfer coefficients

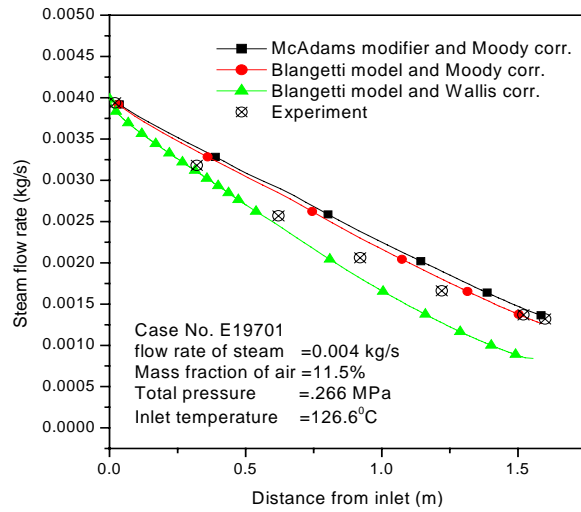


Fig 9 Variation of steam mass flow rate along the length of the tube

### 4.3 Film, condensation and sensible heat transfer coefficients

Figures 15 to 17 show the variation of film heat transfer coefficient, condensation heat transfer coefficient and gas phase sensible heat transfer coefficient for cases E19701, RUN-6.4.1 and RUN-4.4.1. From figures 15 to 17, it can be seen that gas phase heat transfer coefficient is negligible compared to film and condensing heat transfer coefficients. It can also be seen from figure 15, that the condensation heat transfer coefficient is always less than the film heat transfer coefficient. It means the resistance due to gas/vapor boundary layer is controlling the heat and mass transfer as compared to the resistance offered by condensate layer. In figure 16, the analysis with model having McAdams modifier and Moody correlation shows that in the initial length of the tube the condensation heat transfer coefficient is higher compared to film heat transfer coefficient because of high Reynolds number and then it gets reversed after 0.6 m. In the analysis with Blangetti model and Wallis correlation, the condensation heat transfer coefficient is higher than film heat transfer coefficient but the difference between them reduces as the distance from inlet increases.

From figure 17, it can be seen that condensation heat transfer coefficient is always greater than the film heat transfer coefficient and the difference is found to be quite high. So, the resistance due to condensate layer is higher as compared to the resistance offered due to gas/vapor boundary layer. Hence it can be deduced that the resistance due to gas/vapor boundary layer is lower as compared to the resistance due to condensing layer at very high gas/vapor Reynolds number. In general, liquid film becomes thinner with increase in gas flow rate. However, with increase in mixture flow rate, condensation heat transfer increases greatly and liquid film does not become so thinner which can cause further increase in film heat transfer coefficient. Hence, as the inlet mixture Reynolds number increases condensation heat transfer coefficient increases due to the higher turbulence in the gas/vapor boundary layer.

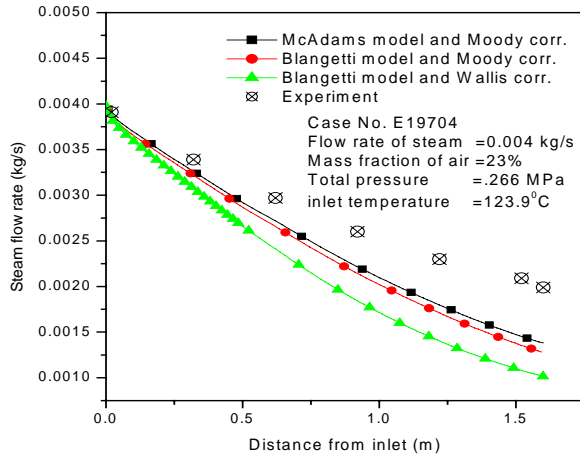


Fig 10 Variation of steam mass flow rate along the length of the tube

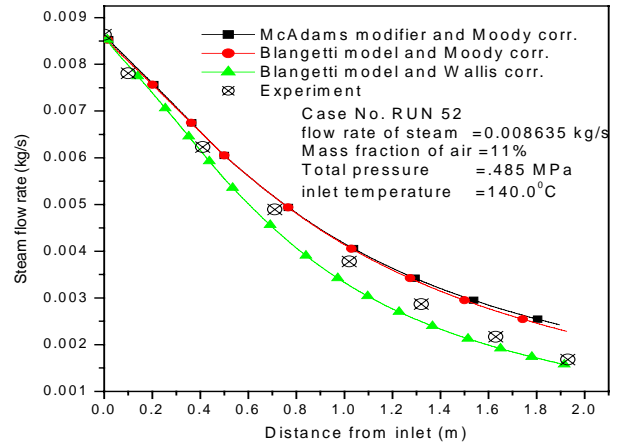


Fig 11 Variation of steam mass flow rate along the length of the tube

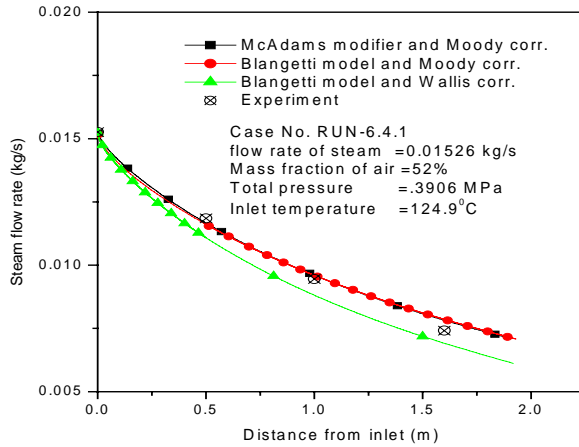


Fig 12 Variation of steam mass flow rate along the length of the tube

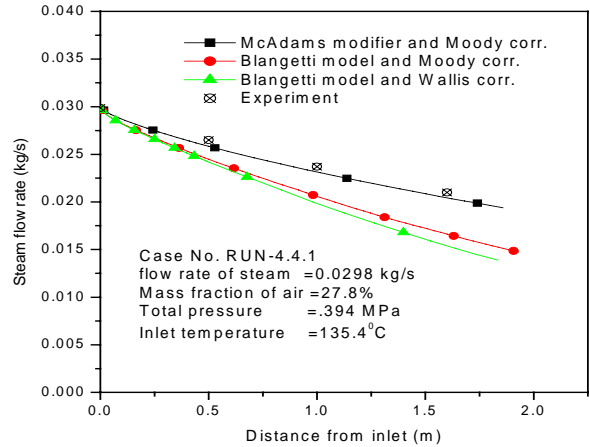


Fig 13 Variation of steam mass flow rate along the length of the tube

It can be seen from figs. 15 to 17 that the heat transfer coefficient for sensible heat transfer from the mixture to liquid film is very small as compared to the other heat transfer coefficients for all the models used in this study. It is almost same value in each case because it is evaluated by Gnielinski correlation for each model.

## 5. CONCLUSIONS

A theoretical model has been developed to study the local heat transfer coefficient of a vapour in the presence of a noncondensable gas, where the gas mixture is flowing downward inside a vertical tube. The model incorporates Nusselt equation with McAdams modifier and Blangetti model for calculating the film heat transfer coefficient, and Moody correlation and Wallis correlation to account for film waviness effect on gas/vapor boundary layer. A comparative study of heat transfer coefficient and steam mass flow rate have been made. Following conclusions can be drawn from this study

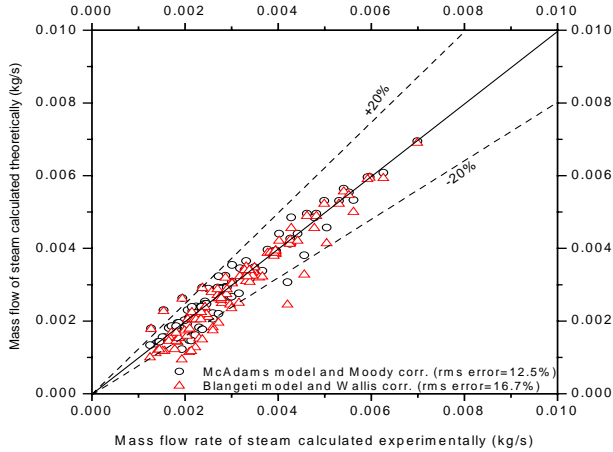


Fig. 14 Comparison between experimental and theoretical steam flow rates inside the tube

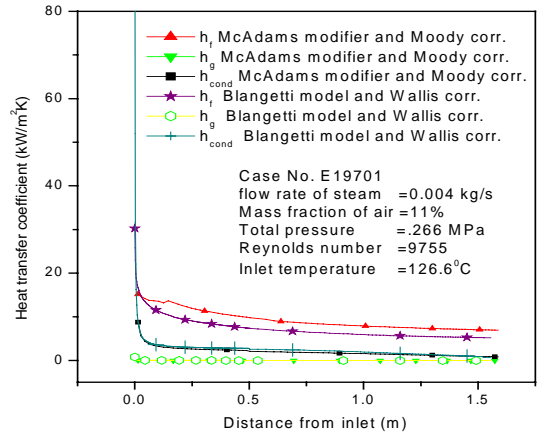


Fig. 15 Variation of heat transfer coefficients along the length of the tube

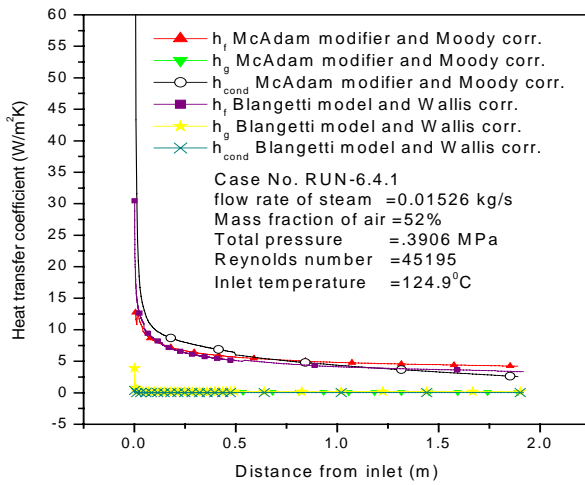


Fig. 16 Variation of heat transfer coefficients along the length of the tube

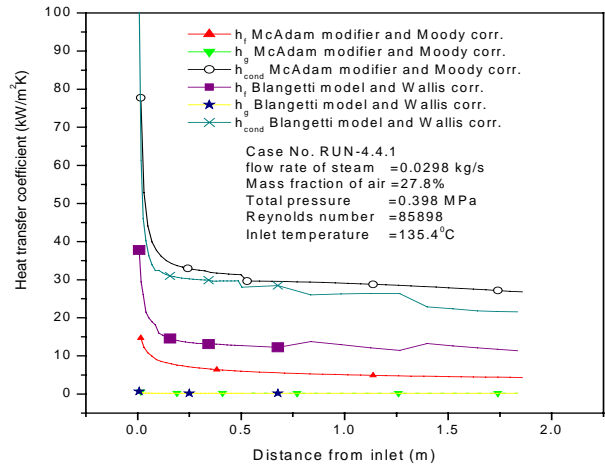


Fig. 17 Variation of heat transfer coefficients along the length of the tube

- The prediction of total heat transfer coefficient by all models is close to the experimental data up to Reynolds number of 90000. The Blangetti model with Wallis correlation predicts higher local heat transfer coefficient compared to those with McAdams modifier and Moody correlation and with Blangetti model and Moody correlation.
- The decrease in mass flow of steam along the length of the tube with Blangetti model and Wallis correlation is more compared to the model with McAdams modifier and Moody correlation and with Blangetti model and Moody correlation. The predicted steam flow rate by the model with McAdams modifier and Moody correlation gives the lowest deviation when compared with Maheshwari's experimental data.
- The thermal resistance offered by gas/vapor boundary layer due to the condensation is higher than that offered by condensing film for low inlet Reynolds number. But this phenomenon may get reversed at higher Reynolds number. As the inlet mixture

Reynolds number increases, the condensation heat transfer coefficient increases due to the higher turbulence in the gas/vapor boundary layer.

## NOMENCLATURE

A	tube inside surface area, $m^2$	Pr	Prandtl number
$B_h$	suction parameter	Q	heat transferred, W
$C_p$	specific heat, J/kgK	$q''$	surface heat flux, $W/m^2$
D	diffusion coefficient, $m^2/s$	R	tube radius, m
d	tube inner diameter, m.	Re	Reynolds number
f	Fanning friction factor	Sc	Schmidt number
$G^\infty$	mixture mass flux, $kg/m^2s$	Sh	Sherwood number
g	acceleration due to gravity, $m/s^2$	St	Stanton number
$H_{fg}$	latent heat of condensation, J/kg	T	temperature, $^\circ C$
h	local heat transfer coefficient, $W/m^2K$	u, v	velocity components, m/s
$h_m$	mass transfer coefficient, $moles/m^2s$	$W^*$	reference mass fraction
k	thermal conductivity, W/mK	W	mass fraction
M	molecular weight	x	distance from tube inlet, m
m	mass flow rate, kg/s	$X^*$	reference partial pressure ratio
$m''$	interfacial mass flux, $kg/m^2s$	y	distance from tube inner wall in radial direction, m
Nu	Nusselt number		
P	pressure, Pa		

## Greek

$\beta$	correction factor
$\delta$	condensate film thickness, m
$\varepsilon$	roughness height, m
$\mu$	absolute viscosity, N-s/ $m^2$
$\rho$	density, $kg/m^3$
$\omega$	noncondensable gas mass fraction ratio in the bulk to that at the liquid/gas interface
$\Gamma$	condensate mass flow rate per unit circumference, $kg/s\ m$
$\tau_g$	interfacial shear stress, $N/m^2$

## Subscripts

b	bulk, noncondensable- steam mixture	o	without suction
cond	condensate	r	rough
f	film	ref	reference
g	gas phase	s	smooth
i	liquid / gas interface	s	steam
in	tube inlet	t	developing
j	step index	tot	total
l	condensed liquid	v	vapour
mix	mixture	w	wall
nc	noncondensable gas	x	local

## REFERENCES

1. Maheshwari N.K., Saha D., Chandraker D.K., Venkat Raj V., Kakodkar A., "Studies on the Behaviour of a Passive Containment Cooling System for the Indian Advanced Heavy Water Reactor", Kerntechnik, Vol. 66, No. 1-2, February 2001.
2. Colburn A.P. and Hougen O.A., "Design of Cooler Condensers for Mixtures of Vapours with Noncondensing Gas," Ind. Eng. Chem., 26, 1178, 1934.

3. Kageyama T., Peterson P.F. and Schrock V.E., "Diffusion Layer Modelling for Condensation in Vertical Tubes with Noncondensable Gases," Nucl. Eng. Design, 41, 289, 1993.
4. Blangetti F., Krebs R., and Schlunder E.U., "Condensation in Vertical tubes- Experimental Results and Modeling", Chemical Engineering Fundamentals, 1, 20-63, 1982.
5. Kageyama T., "Application of Diffusion Layer Theory to Vertical Downflow Condensation Heat Transfer," MS Thesis, University of California, Berkeley, 1992.
6. Vierow K.M., "Behaviour of Steam-Air Systems Condensing in Concurrent Vertical Downflow," MS Thesis, University of California, Berkeley, 1990.
7. Ogg D.G., "Vertical Downflow Condensation Heat Transfer in Gas-Steam Mixtures," MS Thesis, University of California, Berkeley (1991).
8. Siddique M., "The Effects of Noncondensable Gases on Steam Condensation under Forced Convection Conditions," PhD Thesis, Massachusetts Institute of Technology, 1992.
9. Siddique M., Golay M.W. and Kazimi M.S., "Theoretical Modeling of Forced Convection Condensation of Steam in a Vertical Tube in the Presence of a Noncondensable Gas." Nucl. Technology, 106, pp. 202, 1994.
10. Kays W.M. and Moffat R.J., "The Behaviour of Transpired Turbulent Boundary Layers," Studies in Convection", pp. 223, Academic Press, New York, 1975.
11. Ghiaasiaan S.M., Kamboj B.K. and Abdel-Khalik S.I., "Two Fluid Modeling of Condensation in the Presence of Noncondensables in Two Phase Channel Flows." Nucl. Sci. Eng., 119, pp.1, 1995.
12. Hassan Y.A. and Banerjee S., "Implementation of a Noncondensable Model in RELAP5/MOD3", Nucl. Eng. Design, 162, pp. 281, 1996.
13. Siddique M, Golay M.W. and Kazimi M.S., "Local Heat Transfer Coefficients for Forced Convection Condensation of Steam in a Vertical tube in the Presence of a Noncondensable Gas," Nucl. Technology, 102, 386, 1993.
14. Herranz Luis E., Jose L., Munoz-Cobo and Verdu G., "Heat Transfer Modeling in the Vertical Tubes of the Passive Containment Cooling System of the Simplified Boiling Water Reactor", Nuclear Engineering and Design, 178, 29-44, 1997.
15. Gnielinski V., "New Equations for Heat and Mass Transfer in Turbulent Pipe and Channel Flow", Int. Chem. Engg. 16, 359, 1976.

16. No H.C., Park H.S., "Non-iterative Condensation Modeling for Steam Condensation with Non-condensable gas in a Vertical Tube", *Int. J. of Heat and Mass Transfer*, 45, 845-854, 2002.
17. Corradini M.L., "Turbulent Condensation on a Cold Wall in the Presence of a Noncondensable Gas," *Nucl. Technology*, 64, 186, 1984.
18. McAdams W.H., "Heat Transmission", 3rd ed., McGraw-Hill Book Company, New York, 1954.
19. Rohsenow W.M., Webber J.H., and Ling A.T., "Effect of vapor velocity on laminar and turbulent film condensation", Ph.D dissertation, Massachusetts Institute of Technology, 1992.
20. Norris R.H., "Some Simple Approximate Heat Transfer Correlations for Turbulent Flow in Ducts with Rough Surfaces.", *Augmentation of Convective Heat and Mass Transfer*, pp. 66, ASME, New York, 1970.
21. Moody L.F., "Friction Factors for pipe Flow", *Trans. Am. Soc. Mech. Engg.*, 66, 671, 1944.
22. Wallis G.B., *One-dimensional Two Phase Flow*", McGraw-Hill, New York, 1969.
23. Reynolds H.C., Swearingen T.B. and McEligot D.M., "Thermal Entry for Low Reynolds Number Turbulent flow", *J. Basic Eng.*, 91, 87, 1969.
24. Maheshwari N.K., Saha D. Sinha R.K. and Aritomi M., "Experimental Studies on Condensation of Steam Mixed with Noncondensable Gas inside the Vertical Tube in a Pool Filled with Subcooled Water", *Kerntechnik*, vol. 68, 5-6, 2003.
25. Tanrikut A., Yesin O., "Experimental Research on In-Tube Condensation in the Presence of Air", *Proceedings of a Technical Committee Meeting, IAEA TECDOC-1149*, Switzerland, 14-17, September 1998.